Jacek STARZYŃSKI, Jan SROKA

Warsaw University of Technology

Improvement of the E-Field antenna for susceptibility testing

Abstract. *The paper deals wit shape optimization of the E-Field generating antenna for susceptibility testing according to military EMC standard. An optimized antenna shapes allows to minimize the cost of power amplifier used for testing and thus brings substantial economical benefits. The optimal design uses numerical FEM model of antenna and applies Levenberg-Marquardt algorithm to minimize the objective function correlated with non-symmetrical pattern of generated field.*

Streszczenie. *Artykuł przedstawia metodykę optymalnego projektowania anteny generującej pole elektryczne do testów narażeniowych zgodnych z wojskowymi standardami kompatybilności elektromagnetycznej. Zoptymalizowana antena umożliwia zmniejszenie kosztów układu zasilającego przy zachowaniu nie gorszych parametrów generowanego pola elektrycznego. Do optymalnego projektowania wykorzystano algorytm Levenberga-Marquardta i numeryczny model otoczenia anteny wykonany za pomocą metody elementów skończonych.* ***(Optymalne projektowanie anteny generującej pole elektryczne do testów narażeniowych)***

Keywords: EMC, E-Field, susceptibility, numerical model, optimal design
Słowa kluczowe: kompatybilnośc elektromagnetyczna, pole elektryczne, testy narażaniowe, model numeryczny, optymalizacja

The problem

Susceptibility testing according to the military standards includes exposure to E-Field of large intensity and broad frequency range [1]. According to the last and penultimate issues of this standard (F edition: 2007), and (E edition: 1997), exposure frequency range extends from 2MHz to 40GHz, while the range of field strengths range from 10 V/m, by 20 V/m and 50 V/m up to 200 V/m depending on the application in different types of troops. According to an even earlier release of this standard (D edition: 1993), exposure frequency range starts from 10 kHz. There is still market demand for research in the field of 10 kHz.

In this tests, the generating antenna is located 110 cm from the tested object (EUT = Equipment Under Test) placed on a long table (equipment table) with conductive top level (Fig.1.). The minimal size of the shielded room can be estimated as 7×5×3 meters.

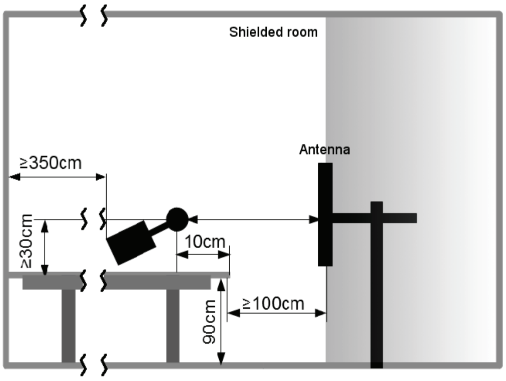

Fig. 1. Test configuration: the power radiated into the shadowed part of the room is useless

In the lower frequency range EUT is placed in the near-field zone in which, to achieve high field intensity, one must apply a high-power antenna and power amplifier. One of the useful antennas on the market is EFG-3B model [2]. This is the 2 kW antenna with frequency range 10 kHz to 220 MHz. Prices of amplifiers in 10 kHz to 1 GHz for 110 W, 400 W and 1100 W are at the level of tens of thousands of dollars and grow by a factor similar to the increase in power (1,0:2,7:9.1).

EFG-3B characteristics is symmetric and thus in a typical test configuration only a half of the amplified power is effectively used—the other part, radiated behind the antenna, can be minimized not affecting the field strength in the EUT.

To change the antenna characteristic a metal patches can be added to the basic construction. The patches will direct field to the front of the antenna. In the optimal design process we search for the shape and position of patches maximizing the electric field strength in the EUT location.

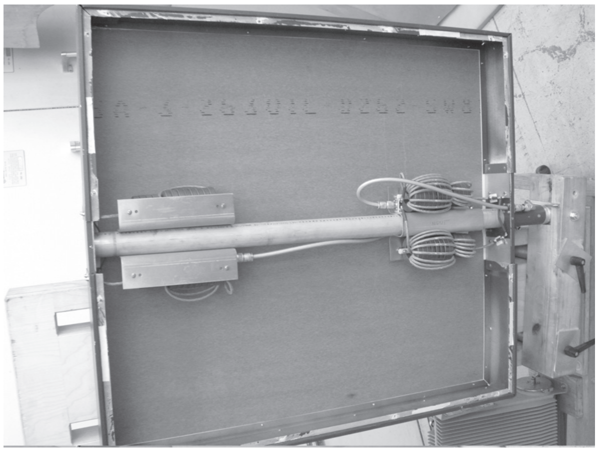

Fig. 2. General view of EFG-3B antenna

The mathematical model

The electric and magnetic fields described by Maxwell equations can be in the case of time-harmonic fields reduced to the vector Helmholtz wave equation [5]. In our problem the domain of interest (Ω) is surrounded by perfect electrical conductors—we shall reference such boundary by Γ_e. The Ω is electrically homogeneous. The wave equation in terms of the electric field, $\mathbf{E}$ can be written as

$$\nabla \times \nabla \times \mathbf{E} - \mathbf{k_o^2}\epsilon_\mathbf{r}\mu_\mathbf{r}\mathbf{E} = \mathbf{0} \qquad \text{in}\boldsymbol{\Omega}, \tag{1}$$

with the boundary condition

$$n \times \mathbf{E} = \mathbf{0} \qquad \text{on} \qquad \text{on}\boldsymbol{\Gamma_e}. \tag{2}$$

ϵ_r and μ_r represent respective the relative permittivity and permeability (both equal 1 in our case) and k_o is the operating wavenumber

$$k_o = \frac{2\pi f_o}{c}, \tag{3}$$

where f_o is the operating frequency and c is the speed of light in free space [6].

For our purpose implementation of the above boundary problem (1),(2) is not sufficient, yet it does not obeys the antenna. We might simulate it using the common procedure described i.e. in [6]. How ever to improve the radiation pattern in the shielded room it is not necessary to make the full 3D, vector field simulation. The preliminary experiments (which will be briefly mentioned later) showed us, that the low frequency range is crucial: if an antenna produces better field for low frequencies, it will operate better in the higher frequencies as well. The “low frequency” means f_o for which the wavelength is much smaller than the antenna size: for EFG-3B it is equivalent to $f_o < 30$ MHz.

To predict the field pattern for the low frequencies it is sufficient to solve the scalar Helmholtz equation for the electric scalar potential

$$\nabla^2 V - k_o^2 \epsilon_r \mu_r V = 0, \tag{4}$$

with the natural boundary condition on the conducting, grounded walls (ant the equipment table)

$$V = 0 \quad \text{on} \quad \Gamma_e \tag{5}$$

and the antenna simulated in form of the boundary conditions

$$V = \pm U \quad \text{on} \quad \Gamma_a, \tag{6}$$

where Γ_a represents the antenna surface.

The numerical model

Numerous numerical methods can be used to solve the (4)-(6) boundary problem. The authors' experience with finite element method was the key factor of the choice.

Using the weighted residual, Galerkin approach allows us to transform the boundary problem (4)-(6) into the following week form

$$\int_\Omega \left(\nabla V \cdot \nabla u - k_o^2 \epsilon_r \mu_r V \cdot u \right) d\Omega = 0, \tag{7}$$

where u is the so-called *test function* [7]. The boundary conditions (5)-(6) are, strictly speaking, enforced to the system of algebraic equations obtained from (7).

Equation (7) can be directly coded into Python or C++ program with help of the Dolfin and FFC components of the FEniCS project [8]. For this paper we have created a Python program, where the weak form of the boundary problem is coded as follows (only the important code snippets are presented):

```
...
# Define boundary conditions
bc = list()
for s in range(3,len(bcdefs)):
  bc.append( DirichletBC(W, ....)

...
# Define variational problem
W = FunctionSpace(mesh, 'CG', 1)
u = TestFunction(W)
v = TrialFunction(W)
f = Constant(0)
mi0 = 4. * pi * 1e-7
eps0 = 1. / 36. / pi * 1e-9
omega = 2. * pi * atof(f_o )
L2 = omega*omega*mi0*eps0
Lambda2 = Constant( L2 )
a = (dot(grad(v), grad(t))
      - Lambda2 * v *t )*dx
L = f*t*dx
V = Function( W )
solve( a == L, V, bc)
...
# post-processing follows
```

In various experiments the field generated by the EFG-3B was simulated by a 2D and 3D finite element models. The frequency range for EFG-3B extends from 10KHz to 220MHz. The EM wave length at 220MHz is 1.36 m what enforces size of the finite element smaller than 13 centimeters. It is obvious that discretization of 7×5×3 m room with such a small elements (we have to remember that in the vicinity of antenna much finer discretization is necessary) will create huge amount of data making models computationally demanding.

The 2D model meshes (different densities up to 162465 nodes and 323447 triangles) were constructed with help of public domain codes: the 2D preprocessor polygen and mesh generator triangle [9]. A very dense mesh with size of triangles smaller than one centimeter allowed for very fine simulation even with linear field approximation over elements. The geometry of the 2D model is shown in Fig. 3—comparing it with Fig. 1, the reader will recognize the basic elements: the table (T), the antenna cross-section (A1 and A2) and the EUT location.

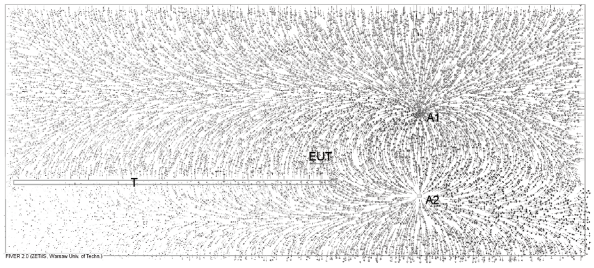

Fig. 3. The geometry of the 2D model and $\mathbf{E}$ (magnitudes are in logarithmic scale) at f_o =10 MHz

The E for operating frequency 10 MHz is also presented on Fig.3. Logarithmic scale was used to show the field direction, because the relative values of $|E|$ far from the antenna are of course very small at this frequency: $k_o^2 \approx 0.44$ and the wave effects may be neglected in (1). Fig. 4 shows relative magnitude of $\mathbf{E}$ ($20\log(|E|/max|E|)$) over the model. The logarithmic scale was narrowed to [-120dB. . . -40dB] range to score under the variation of $\mathbf{E}$ at the EUT location.

Fig. 4. $20log(\frac{|E|}{max|E|})$ at f_o =10 MHz; gray-scale: -120dB (black) ÷ -40dB (white)

Similar picture (notify the scale change) for $f_o = 100$ MHz is shown in Fig. 5—the wave effects are clearly visible at this frequency ($k_o^2 \approx 4.39$).

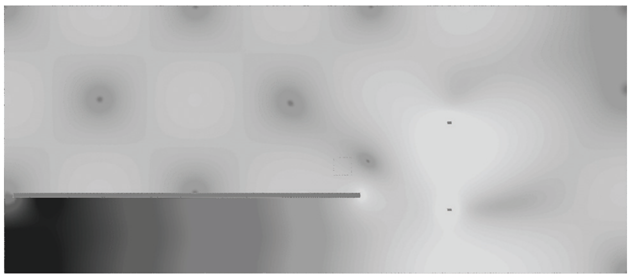

Fig. 5. $20log(\frac{|E|}{max|E|})$ at f_o =100 MHz; gray-scale: -120dB (black) ÷ -20dB (white)

The geometry of 3D model is shown in Fig. 6. Only a half of the shielded room was simulated with the homogeneous Neumann boundary condition set on the symmetry plane.

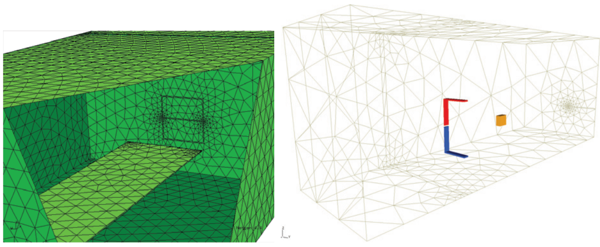

Fig. 6. The 3D model: view of the antenna arrangement from the EUT side and general geometry of the FE model (only the antenna and ETU-zone shown, rough FE mesh is used to clarify the view) used for calculations

The density of 3D mesh varied up to 78846 nodes and 422178 elements. The simulation time was approximately 10 times longer than for 2D model an thus we use the 2D simulator for optimal design and 3D model for validation only.

The results

The optimizer was based on the levmar library [4] implementing the Levenberg-Marquardt algorithm. We have optimized the length and angle of two reflectors mounted on the upper and lover part of the antenna. The optimal shape, increasing field intensity in the EUT zone by factor at least 3 (at 10 kHz) is shown in Fig. 7 (right inset) compared to the original antenna shape.

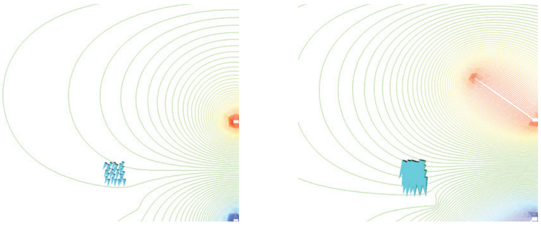

Fig. 7. The original (left) and optimized (right) antenna: electric potential the EUT location (the same intervals between the equipotential lines)

The modified antenna was better at the whole operating frequency range. It is shown in Fig. 8, showing the relative magnitude of the field intensity. The directed radiation pattern is clearly visible in Fig. 9, comparing electric field in the 2D model at f_o =100 MHz for the original antenna and for the modified one in two orientation: towards the table and towards the opposite wall.

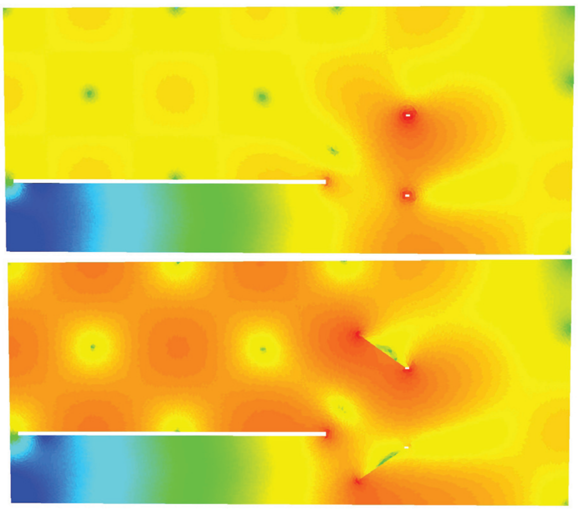

Fig. 8. $20log(|E|/|E|_{max})$ for f_o=100MHz: original antenna (top) and the modified one (bottom)

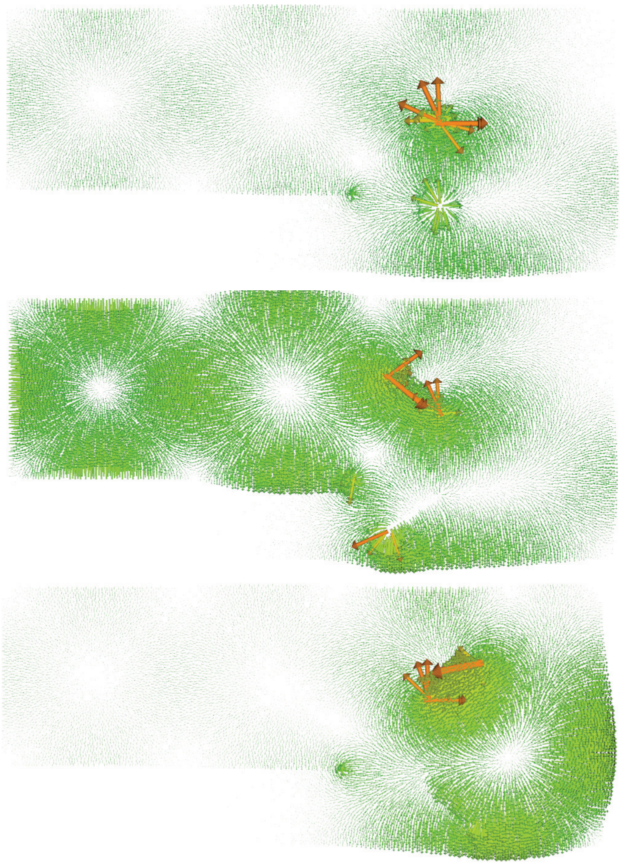

Fig. 9. The original (top) and optimized (middle and bottom) antenna: electric field strength in the 2D model

Conclusion

The simplified models presented in this paper allowed us to increase the field strength by the factor 3 comparing to the original antenna shape.

Acknowledgment: We wish to offer a special acknowledgement to dr. Robert Szmurło, the author of polygen and fiver programs, used for FE pre- and post-processing.

REFERENCES

[1] Department of Defense Interface Standard, Requirements for the Control of Electromagnetic Interference Characteristics of Subsystems and Equipment, MIL-STD-461F: 2007

[2] EFG-3/EFG3B Series, Instruments for Industry INC, Application Note, Available at `http://www.ifi.com`

[3] J. Sroka: Niepewność pomiarowa w badaniach EMC, pomiary emisyjności radioelektrycznej, Oficyna Wydawnicza Politechniki Warszawskiej, Warszawa 2009,

[4] M.I.A. Lourakis, levmar: Levenberg-Marquardt nonlinear least squares algorithms in C/C++, available at `http://www,ics,forth,gr/~lourakis/levmar/`, Jul, 2004

[5] J. Jin: Theory and Computation of Electromagnetic Fields, Willey-IEEE Press, 2010

[6] J. Jin, D. J. Riley: Finite Element Analysis of Antennas and Arrays, Willey-IEEE Press, 2009

[7] H.P. Langtangen: Computational Partial Differential Equations, 2nd Edition, Springer 2003

[8] FEniCS Team: FEniCS Project Home Page `http://fenicsproject.org`, 2011

[9] J.R. Shevchuk: Triangle: Engineering a 2D Quality Mesh Generator and Delaunay Triangulator, in volume 1148 of LNCS, pages 203-222, Springer-Verlag, Berlin, May 1996.

Authors: Jacek Starzyński, Jan Sroka, Institute of Theory of Electrical Engineering, Measurement and Information Systems, Faculty of Electrical Engineering, Warsaw University of Technology, ul. Koszykowa 75, 00-662 Warszawa, Poland, email: jstar@iem.pw.edu.pl